

# Large Multimodal Model Compression via Efficient Pruning and Distillation at AntGroup

Maolin Wang\*<sup>†</sup>  
City University of Hong Kong  
Hong Kong SAR, China  
morin.wang@my.cityu.edu.hk

Yao Zhao\*  
AntGroup  
Hangzhou, China  
nanxiao.zy@antgroup.com

Jiajia Liu  
AntGroup  
Hangzhou, China  
lekun.ljj@antgroup.com

Jingdong Chen  
AntGroup  
Hangzhou, China  
jingdongchen.cjd@antgroup.com

Chenyi Zhuang  
AntGroup  
Hangzhou, China  
chenyi.zcy@antgroup.com

Jinjie Gu  
AntGroup  
Hangzhou, China  
jinjie.gujj@antgroup.com

Ruocheng Guo  
ByteDance Research  
London, UK  
rguo.asu@gmail.com

Xiangyu Zhao  
City University of Hong Kong  
Hong Kong SAR, China  
xianzhao@cityu.edu.hk

## ABSTRACT

The deployment of Large Multimodal Models (LMMs) within AntGroup has significantly advanced multimodal tasks in payment, security, and advertising, notably enhancing advertisement audition tasks in Alipay. However, the deployment of such sizable models introduces challenges, particularly in increased latency and carbon emissions, which are antithetical to the ideals of Green AI. This paper introduces a novel multi-stage compression strategy for our proprietary LLM, AntGMM. Our methodology pivots on three main aspects: employing small training sample sizes, addressing multi-level redundancy through multi-stage pruning, and introducing an advanced distillation loss design. In our research, we constructed a dataset, the Multimodal Advertisement Audition Dataset (MAAD), from real-world scenarios within Alipay, and conducted experiments to validate the reliability of our proposed strategy. Furthermore, the effectiveness of our strategy is evident in its operational success in Alipay’s real-world multimodal advertisement audition for three months from September 2023. Notably, our approach achieved a substantial reduction in latency, decreasing it from 700ms to 90ms, while maintaining online performance with only a slight performance decrease. Moreover, our compressed model is estimated to reduce electricity consumption by approximately 75 million kWh

annually compared to the direct deployment of AntGMM, demonstrating our commitment to green AI initiatives. We will publicly release our code and the MAAD dataset after some reviews<sup>1</sup>.

## KEYWORDS

Large Language Model, Large Multimodal Model, Model Compression, Pruning, Distillation, Efficient Inference

### ACM Reference Format:

Maolin Wang, Yao Zhao, Jiajia Liu, Jingdong Chen, Chenyi Zhuang, Jinjie Gu, Ruocheng Guo, and Xiangyu Zhao. 2023. Large Multimodal Model Compression via Efficient Pruning and Distillation at AntGroup. In *Proceedings of (Arxiv Preprint)*. ACM, New York, NY, USA, 11 pages. <https://doi.org/XXXXXXX.XXXXXXX>

## 1 INTRODUCTION

The advent of Large Language Models (LLMs) [3, 4, 36, 41] marks a significant milestone in Artificial Intelligence (AI). An even broader paradigm, the Large Multimodal Model (LMM) [21, 29, 45], expands the capabilities of LLMs by incorporating visual signals. LMMs excel not only in handling and generating substantial textual-only tasks, but also demonstrate impressive performance in various multimodal tasks, such as video recommendations [43], image understanding [1], and dialogue systems [6]. Particularly within our AntGroup, a leading technology company specializing in financial services and digital payments, LMMs have achieved significant improvements in multimodal tasks related to video-text comprehension and image-text comprehension in our platform and advertising sectors. Specifically, in the scenarios of short video categorization on Alipay, a platform renowned in China for its extensive financial services and digital payment solutions, we observed a notable 4.2% enhancement in the accuracy of primary category classification. Regarding the multimodal advertisement audition task on the same platform, we recorded a substantial 18.7% increase in attribute recognition accuracy. Furthermore, LMMs have demonstrated a significant improvement in digital advertising effectiveness, evidenced

\*Both authors contributed equally to this research.

<sup>†</sup>All work performed during internship at AntGroup

Permission to make digital or hard copies of all or part of this work for personal or classroom use is granted without fee provided that copies are not made or distributed for profit or commercial advantage and that copies bear this notice and the full citation on the first page. Copyrights for components of this work owned by others than ACM must be honored. Abstracting with credit is permitted. To copy otherwise, or republish, to post on servers or to redistribute to lists, requires prior specific permission and/or a fee. Request permissions from [permissions@acm.org](mailto:permissions@acm.org).

*Arxiv Preprint*,

© 2023 Association for Computing Machinery.  
ACM ISBN 978-x-xxxx-xxxx-x/YY/MM...\$15.00  
<https://doi.org/XXXXXXX.XXXXXXX>

<sup>1</sup>[https://github.com/MorinW/AntGMM\\_Pruning](https://github.com/MorinW/AntGMM_Pruning)

by a 1.4% rise in Click-Through Rate (CTR) and a remarkable 34% uplift in Per-View Click-Through Rate (PVCTR) in the context of video topic voting scenarios.

Despite the remarkable capabilities of LMMs, their deployment in particular business frameworks, such as AntGroup’s multimodal advertisement audition tasks, poses significant challenges. Predominantly, the extensive size of these models necessitates substantial computational and storage resources [49], consequently leading to increased latency—from approximately 85ms to 700ms—in the context of AntGroup’s multimodal advertisement audition tasks, thereby considerably deteriorating user experience. Moreover, the direct implementation of LMM is associated with significant electricity consumption, a pressing concern in the quest for environmentally sustainable AI solutions. This quest aligns with AntGroup’s objectives of advancing Green AI [47], a movement aimed at fostering ecological integrity and social justice throughout the AI product lifecycle. A critical challenge in addressing these aspects lies in striking a balance between maintaining model performance and reducing energy and time consumption [47]. Model compression [49] emerges as a promising avenue to ameliorate LMM’s inference efficiency and curtail electricity consumption without substantial compromises, thereby paving the way for more sustainable and user-centric AI solutions.

In recent years, the academic discourse has illuminated several techniques to tackle the model compression issues, centralizing on methodologies such as model pruning [11, 23], knowledge distillation [15, 34], and quantization [16, 30]. Nevertheless, the majority of the existing literature [40] on transformer model compression is predominantly anchored in the BERT-style pre-training and fine-tuning paradigm. These compression strategies are primarily tailored for natural language understanding (NLU) tasks and exhibit a lack of direct applicability to the contemporary generative LMMs [49].

For compressing generative decoder-only LLMs, we believe there are the following distinct challenges:

- (1) **Challenge 1: Retraining LLMs is Cost-prohibitive.** Many earlier compression techniques depended on extensive retraining over large corpora [40]. However, as LLMs or LMMs [3, 4, 36, 41] have scaled the corpus size to trillions of tokens or more, retraining has become infeasible.
- (2) **Challenge 2: Identifying Multi-level Redundancy is Difficult.** Boasting a parameter count of at least 1 billion or more alongside an intricate structure, the redundancy within LLMs or LMMs is apparent at multiple levels, encompassing **the number of blocks, input dimensions, and intermediate-module dimensions**. Addressing redundancy across these levels in one shot will result in a non-smooth impact on performance [35].
- (3) **Challenge 3: Sequential Token Generation Complicate Compression Task.** Generating extended texts is inherently challenging due to the cascading nature of the task, where each step entails large-scale classification (e.g., a vocabulary size of over 100,000 implies more than 100,000 categories). A divergence from the ground truth for a single token during generation can cause subsequent tokens to deviate considerably. It’s worth noting that the loss during the distillation phase requires the specialized design to address these challenges effectively.

Although efforts have explored the application of unstructured pruning [10, 33], structured pruning, [9, 26] or knowledge distillation techniques to generation task [12, 32], existing works cannot address three challenges above. In alignment with the objectives of Green AI and to enhance efficiency, we introduce a multi-stage compression strategy aimed at optimizing and amplifying the advantages of our pre-trained LMMs, namely the Antgroup General Multimodal Model (AntGMM). To address the aforementioned challenges, our primary innovations:

- (1) **Finetuning on Small Dataset:** Notably, we start with the parameters of the original network. We then alternate between structure pruning and knowledge distillation to ensure a minor loss in performance. Given our strategy of inheriting parameters from the original network and performing asynchronous pruning and distillation (finetuning), our method does not require an extensively large dataset for retraining.
- (2) **Tackling Multi-level Redundancy through Multi-stage Pruning:** To mitigate the inherent redundancy in LMMs, we will introduce a multi-stage pruning methodology. This multi-stage approach streamlines the Pruning process by addressing redundancies across various aspects, such as the number of layers, module hidden dimensions, and module input dimensions. Consequently, our method ensures consistent performance while achieving improved inference efficiency.
- (3) **A Novel Distillation Loss for Generation Task:** To address the complexities inherent in generative tasks, we crafted a loss distillation function that takes into account both token accuracy and contextual appropriateness. Specifically, beyond aligning model output logits, we introduced a pairwise loss to encourage correct responses. This is achieved by constraining the logit values of correct answers to be greater than the most top logit.

Our framework has been operational in Alipay’s multimodal advertisement audition scenario for **three months**, commencing from **September 2023**. Significantly, our framework not only maintained online performance, with only a marginal decrease of 0.8% in the seven-day average accuracy, but also significantly reduced latency, cutting it down from **700ms** to **90ms**. Simultaneously, in comparison to the direct deployment of the AntGMM, our compressed model is projected to reduce electricity consumption by approximately **75 million kWh** annually. This substantial decrease stands as a testament to a commitment to pursuing green AI.

## 2 PRELIMINARY

### 2.1 AntGMM: Ant Group’s Foundational LMM

At Ant Group, we have developed and pre-trained a proprietary LMM, termed Antgroup General Language Model (AntGMM). The current version of AntGMM adopts a BLIP-2-like [21] architecture that facilitates the integration of a multimodal base model, the AntGMM Encoder, with a comprehensive NLP model, termed as Antgroup General Language Model (AntGLM). As illustrated in Figure 1, AntGMM bridges the modality divide utilizing a novel Querying Transformer (Q-Former) subjected to a dual-stage pre-training process. It first partakes in vision-language representation learning using a static image encoder and subsequently transitions to a vision-to-language generative learning stage leveraging a static large language model. The AntGLM is pre-trained on a blend of

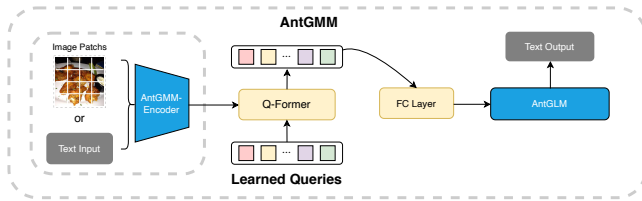


**Figure 1: Model structure of concurrent version of AntGMM. We adopted a structure akin to BLIP-2 as the cornerstone within the Ant Group.**

public datasets and an extensive corpus of proprietary business data. To enhance business relevance, the AntGMM Encoder and the Q-Former have been pre-trained on our internal datasets. The AntGMM is the foundation of Ant Group’s multimodal business applications, marking a notable step in bringing together visual and textual data, thus enabling more intuitive and enhanced interactions in business-focused applications. It should be noted that the AntGMM architecture is subject to ongoing iterative refinements aligned with business requirements. In this paper, we will only focus on the early version of the AntGMM.

## 2.2 Structured Pruning of Neural Networks

Structured pruning [2, 26] is a methodology that aims at mitigating the computational and memory overhead associated with neural networks, which is of paramount importance for models deployed on resource-constrained devices. Unlike unstructured pruning [10, 17] that relies on sparse operations, structured pruning entails the removal of entire neurons or layers from the neural network. This leads to a model with a reduced architecture that is better suited for hardware accelerations [19]. The objective of structured pruning can be succinctly formulated as an optimization problem: For a neural network  $f$  characterized by a weight tensor  $W$ , the aim of structured pruning is to identify a more compact network  $g$  with a reduced weight tensor  $W'$ . This reduction in the network’s size should incur minimal performance loss  $\Delta P(\mathcal{D})$  on a dataset  $\mathcal{D}$ . The performance decrement is defined as the absolute difference in a performance metric  $P$ , such as cross-entropy, between the full and pruned networks:  $\Delta P(\mathcal{D}) = |P(f, \mathcal{D}) - P(g, \mathcal{D})|$ . To ascertain the significance of each parameter in  $f$  and decide which ones to prune to get  $g$ , various criteria are employed by different structured pruning strategies. These often include the magnitude of weights to gauge each parameter’s importance [28]. In this paper, we adopt a structured pruning strategy that leverages a first-order approximation to guide our pruning decisions.

## 2.3 Knowledge Distillation

Knowledge Distillation (KD) [12, 13, 32] is a prominent model compression technique where a compact and efficient student neural network  $g$  is trained to replicate the behavior of a larger, pre-trained teacher neural network  $f$ . In the seminal KD framework proposed by Hinton [13], the distillation procedure entails an optimization process where the student network minimizes a composite loss function. This function is a combination of a ground truth loss  $\mathcal{L}_{CE}(g(x), y)$  and a fidelity loss  $\mathcal{L}_{KD}(g(x), f(x))$ , where  $x$  denotes

**Table 1: Notations used in our algorithm**

Symbol	Description
$f$	LMM model
$g$	Pruned LMM model
$\mathcal{D}_p$	Pruning dataset
$\mathcal{D}_d$	Distillation dataset
$\mathcal{D}_t$	Test dataset
$\alpha$	Maximum performance tolerance
$E$	Number of post-distillation epochs
$N_{blocks}$	Maximum number of pruned blocks
$n_b$	Number of blocks pruned at each step
$N_{inter}$	Maximum reduction in Inter-Module Dimensions
$n_h$	Number of Inter-Module Dimensions pruned at each step
$N_{input}$	Maximum reduction in input dimensions
$n_d$	Number of input dimensions pruned at each step

the input data and  $y$  represents the corresponding ground truth labels. However, further investigations in the realm of Natural Language Processing (NLP) have demonstrated that exclusively focusing on soft aligning via fidelity loss  $\mathcal{L}_{KD}(g(x), f(x))$  can enhance the student model’s performance [25, 46]. For straightforward classification tasks, this distillation loss can be operationalized by aligning the logit outputs of the teacher and student models through the Kullback-Leibler (KL) divergence [31]. Nonetheless, when addressing the intricacies of generative tasks, reliance on KL divergence alone proves to be inadequate for LMMs [12]. We designed a pair-wise loss approach to recover performance.

## 3 METHODOLOGY

In this section, we will present our compression algorithm in detail. The parameter notations of this paper are detailed in Table 1.

### 3.1 Overview

In this subsection, we detail a systematic approach to efficiently prune an LMM to reduce its size without significant performance degradation. The overarching procedure, illustrated in Algorithm 1, is compartmentalized into three main stages to ensure a structured reduction process. 1) Firstly, the *Block Pruning* stage focuses on the initial reduction of the LMM’s block numbers. This stage pruned several last blocks within the LMM. 2) Subsequently, the *Inter-Module Dimension Pruning* phase refines the structure further by targeting the Feedforward Networks (FFNs) and Attention mechanisms within the LMM. This entails a granular optimization where the dimensions within blocks are assessed and pruned. 3) The final stage, *Input-Dimension Pruning*, adjusts the input sizes for each block in the model. It carefully resizes the input dimensionality of every block to match the pruned structure, allowing the LMM to operate more efficiently without incurring unnecessary computational costs associated with processing oversized inputs. Throughout the pruning stages, the model is subjected to performance thresholds that prevent the pruning process from degrading the model’s accuracy beyond an acceptable level. Additionally, to compensate for any potential loss in performance due to the reduction in model complexity, every pruning process is interspersed with several distillation epochs. This approach promises a balance between model

---

**Algorithm 1: Language Multimodal Model Pruning Procedure**


---

**Input:**  $f, \mathcal{D}_p, \mathcal{D}_d, \mathcal{D}_t, \alpha, E, N_{blocks}, N_{inter}^{(Att)}, N_{inter}^{(FFN)}, N_{input}, d, n_b, n_h^{(FFN)}, n_h^{(Att)}, n_d$   
**Output:** Pruned model  $g$

- 1 Calculate performance  $p_f$  of  $f$  using  $\mathcal{D}_d$
- 2 Initialize pruned LMM  $g_0 \leftarrow f$
- /\* Stage 1: Block Pruning \*/
- 3 **while**  $p_f - p_{g_0} < \alpha$  **and** Not reached maximum number of pruned blocks  $N_{blocks}$  **do**
- 4     Remove the last  $n_b$  block from the largest module in  $g_0$
- 5     Distill  $g_0$  for  $E$  epochs using loss from Eq. 5 and  $\mathcal{D}_d$
- 6     Calculate current performance  $p_{g_0}$  with  $\mathcal{D}_d$
- 7  $g_1 \leftarrow g_0$
- /\* Stage 2.1: Inter-Module Pruning in FFN \*/
- 8 **while**  $p_{g_0} - p_{g_1} < \alpha$  **and** Not reached maximum Inter-Module Dimension reduction  $N_{inter}^{(FFN)}$  **do**
- 9     **for** each block in  $g_1$  **do**
- 10         Prune  $n_h^{(FFN)}$  hidden dimensions of FFN via Eq. 2
- 11         Distill  $g_1$  for  $E$  epochs via Eq. 5 and  $\mathcal{D}_d$
- 12         Calculate current performance  $p_{g_1}$  with  $\mathcal{D}_d$
- 13  $g_2 \leftarrow g_1$
- /\* Stage 2.2: Inter-Module Pruning in Att \*/
- 14 **while**  $p_{g_1} - p_{g_2} < \alpha$  **and** Not reached maximum Inter-Module Dimension reduction  $N_{inter}^{(Att)}$  **do**
- 15     **for** each block in  $g_2$  **do**
- 16         Prune  $n_h^{(Att)}$  hidden dimensions in Att via Eq. 3
- 17         Distill  $g_2$  for  $E$  epochs using loss from Eq. 5 and  $\mathcal{D}_d$
- 18         Calculate current performance  $p_{g_2}$  with  $\mathcal{D}_d$
- 19  $g_3 \leftarrow g_2$
- /\* Stage 3: Input/Output Dimension Pruning \*/
- 20 **while**  $p_{g_2} - p_{g_3} < \alpha$  **and** Not reached maximum input-dimension reduction  $N_{input}$  **do**
- 21     Prune  $n_d$  input/out dimensions using Eq. 4
- 22     Distill  $g_3$  for  $E$  epochs using loss from Eq. 5 and  $\mathcal{D}_d$
- 23     Calculate current performance  $p_{g_3}$  with  $\mathcal{D}_d$
- 24 **return**  $g \leftarrow g_3$

---

efficiency and performance, making deploying LMMs more practical in resource-constrained environments.

### 3.2 Element-wise Importance Calculation

In the realm of neural network pruning, traditional metrics such as the L1 norm [44] or magnitude-based approaches [18] are foundational. They provide a direct and sensitive means to assess the impact of individual weights on network performance. Within this domain, first-order and second-order techniques are of particular significance. First-order [14] gradients are of considerable importance in this context. They offer insightful reflections on the influence of weight modifications on the loss function. This is especially

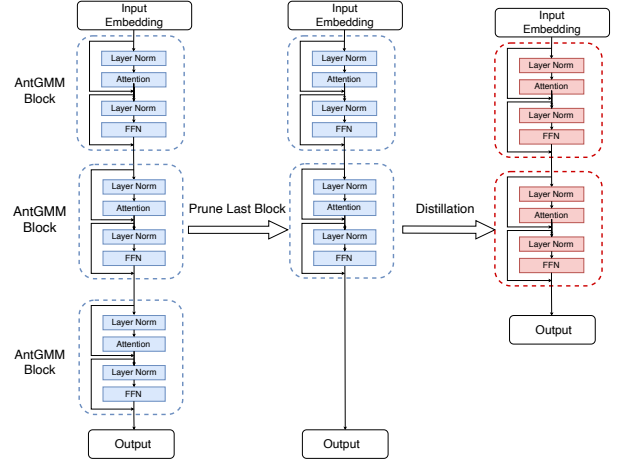


**Figure 2: Block pruning. Block pruning involves removing the last layer (or a few last layers) at each iteration, followed by distillation to ensure minimal loss in model performance.**

relevant in scenarios with limited data availability, where a direct evaluation of each weight’s contribution is essential [38].

Motivated by these challenges, we have utilized first-order gradient information to estimate the importance of weights. Suppose given a small dataset  $\mathcal{D} = \{X, Y\}$ , the importance of one specific parameter  $\theta$  in the neural network  $f$  can be formulated as:

$$I_\theta = |\Delta \mathcal{P}(\mathcal{D})| = |\mathcal{P}_f(\mathcal{D}) - \mathcal{P}_{f_{\theta=0}}(\mathcal{D})| \approx \left| \frac{\partial \mathcal{P}_f(\mathcal{D})}{\partial \theta} \theta + \mathcal{O}(|\theta|^2) \right| \quad (1)$$

where  $f_{\theta=0}$  represents the neural network in which the specific parameter  $\theta$  has been pruned, i.e., assigned  $\theta$  a value of zero. Evaluation of  $P$  can be articulated through the loss function  $\mathcal{L}$ , the deviation  $|\frac{\partial \mathcal{L}(\mathcal{D})}{\partial \theta} \theta|$  can serve as a proxy for assessing the importance of the single parameter  $\theta$ .

### 3.3 Multi-stage Pruning

Facing the intricate challenge of multi-level redundancy in large models with billions of parameters, our research introduces a multi-stage pruning approach to systematically enhance efficiency while maintaining model performance.

**3.3.1 Stage 1: Block Pruning.** As depicted in Figure 2, our methodology initiates by pruning blocks to reduce model complexity, thereby decreasing its depth. Our process begins with removing the final block, followed by iterative model distillation until convergence is achieved. This step is repeated—each time removing an additional block—until a significant increase in loss is detected. The total parameter count of the models is directly tied to the remaining number of blocks; hence, directly reducing blocks results in a substantial decrease in model complexity. However, this is the coarsest level of granularity and has a considerable impact on the effectiveness of the model.

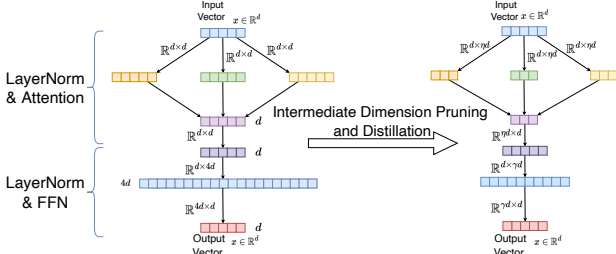


**Figure 3: Intermediate-module dimension pruning. The second stage focuses on dimensionality pruning of the hidden layers of FFNs and attention mechanisms within blocks.**

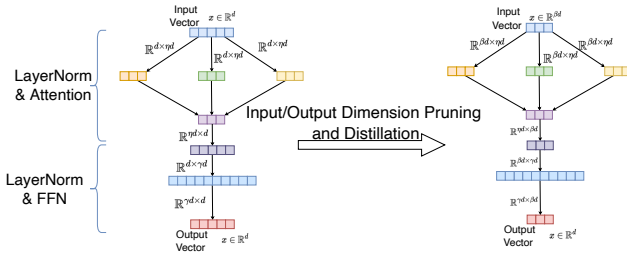


**Figure 4: Input dimension pruning. The final stage reduces the number of parameters associated with both the input and output dimensions. This requires synchronized reduction across all AntGMM blocks.**

**3.3.2 Stage 2: Inter-Module Dimension Pruning.** In the second stage of our process, as shown in Figure 3, we concentrate on dimensionality reduction of the hidden layers via a combination of pruning and knowledge distillation. This stage focuses on the Inter-Module Dimensions of feed-forward networks (FFNs) and attention mechanisms within AntGMM blocks, identifying and pruning redundant parameters based on their calculated importance.

To ascertain the significance of each Inter-Module Dimension, which is associated with many parameters, we aggregate the importance by summation. The importance of the  $n$ -th Inter-Module Dimension in an FFN,  $y = \text{FFN}(x) = (\mathbf{W}^{(\text{out})})\text{GELU}(\mathbf{W}^{(\text{in})}x)$ , with parameters  $\mathbf{W}^{(\text{out})} \in \mathbb{R}^{4d \times 4d}$  and  $\mathbf{W}^{(\text{in})} \in \mathbb{R}^{d \times 4d}$ , is computed as:

$$I_{\text{inter}}^{(\text{FFN})}(n) = \sum_{i=1}^d I(\mathbf{W}_{in}^{(\text{in})}) + \sum_{j=1}^{4d} I(\mathbf{W}_{nj}^{(\text{out})}), \quad (2)$$

where  $I(\cdot)$  denotes the importance measure as defined in Eq. 1,  $d$  is the dimension number of input vectors.

Regarding the attention mechanism, the importance of the  $n$ -th dimension in  $h$ -th head is calculated using the significance of the attention operation parameters  $\mathbf{W}_h^{(Q)}$ ,  $\mathbf{W}_h^{(K)}$ , and  $\mathbf{W}_h^{(V)}$ , along

with the attention projecting parameters  $\mathbf{W}_h^{(O)}$ , as follows:

$$I_{\text{inter}}^{(\text{Att})}(n) = \sum_h \sum_{i=1}^d \left( I(\mathbf{W}_{hin}^{(Q)}) + \sum_{j=1}^d I(\mathbf{W}_{hin}^{(K)}) + \sum_{k=1}^d I(\mathbf{W}_{hin}^{(V)}) + \sum_{l=1}^d I(\mathbf{W}_{hnl}^{(O)}) \right). \quad (3)$$

The pruning of each block is conducted independently, yet for the sake of uniformity, we ensure that the dimension pruned in each block is consistent in every iteration. Pruning and distillation are performed iteratively until a significant loss in performance is noted. This results in reduced dimensions of the weight matrix, particularly adjacent to the output layer. As illustrated in Figure 3, this stage effects a substantial reduction in the parameters.

**3.3.3 Stage 3: Input/Output Dimension Pruning.** In the final stage, as shown in Figure 4, we concentrate on reducing the number of parameters associated with input and output dimensions, we concentrate on reducing the number of parameters associated with input and output dimensions. Unlike Inter-Module Dimension pruning, pruning the input/output dimension necessitates synchronized reduction across all blocks and associated modules (this includes the embedding module, layer normalization, attention, and FFNs) to ensure dimension consistency. Specifically, for the  $n$ -th input/output dimension, its importance is defined as:

$$I^{(\text{In/Out})}(n) = \sum_b \left( \sum_i I(\mathbf{W}_{ni}^{(b)(\text{in})}) + \sum_j I(\mathbf{W}_{jn}^{(b)(\text{out})}) + \sum_h \left( \sum_k I(\mathbf{W}_{hnk}^{(b)(Q)}) + \sum_l I(\mathbf{W}_{hnl}^{(b)(K)}) + \sum_p I(\mathbf{W}_{hnp}^{(b)(V)}) + \sum_q I(\mathbf{W}_{hqn}^{(b)(O)}) \right) \right), \quad (4)$$

where  $\mathbf{W}^{(b)}$  represents the parameters within the  $b$ -th block. It is noteworthy that parameters across all blocks are pruned. Hence, this stage culminates in a reduction in the size of all weight matrices, significantly compressing the model. As depicted in Figure 4, this phase achieves a further decrement in the number of parameters.

### 3.4 Distillation Loss Design

Addressing the complexity of sequential token generation in text synthesis, where even a single token deviation can cascade into significant errors, we innovate on distillation loss design to optimize compression in large-scale language models.

Specifically, in the distillation phase for generative models, we address the complexity of sequential token generation by introducing a pairwise loss function. This key element of our approach ensures prioritization of the logits for correct token responses over those for incorrect tokens, thereby explicitly enhancing the model's ability to generate contextually accurate responses. The distillation

loss function is defined as:

$$\mathcal{L}_{distill} = \sum_{i=1}^{\text{Length}} (\text{KL}(g_i(x), f_i(x)) + \gamma \max(0, \text{Prob}_f^i(\text{Token} = T_i^g) - \text{Prob}_g^i(\text{Token} = T_i^g))) \quad (5)$$

where Length signifies the maximum token length in the sequence,  $T_i^g$  is the token with the highest probability for  $g$  at the  $i$ th position,  $\gamma$  is a hyperparameter that balances the pairwise loss, and  $\text{Prob}_g$  denotes the probability that network  $g$  assigns to a specific token at the  $i$ th position. This function aims to minimize the KL divergence between the probability distributions of the teacher and student networks while ensuring that the student’s confidence in predicting the actual tokens is at least on par with the teacher’s. The pairwise loss element in our approach addresses the tendency of the model to make frequent but incorrect predictions by adjusting the logits. This ensures that the logits for the correct answers could surpass those for the most incorrect answers. Implementing this mechanism effectively lowers the chance of consistent incorrect responses, fostering a more precise and appropriate generation.

## 4 EXPERIMENTS

In the context of multimodal scenarios, pre-training of image semantics is a prerequisite. However, for the specific task of multimodal advertisement auditing, we face a unique challenge: the absence of both a **dedicated open dataset** and a **baseline model with appropriately aligned semantics**. To overcome this, we constructed a multimodal advertisement auditing dataset from our own business and exclusively employed our pre-trained model, AntGMM. This model was specifically developed to meet the unique requirements of this task. In this section, we will conduct experiments on our ad-auditing dataset to answer the following research questions.

- **RQ1:** What is the performance at each stage?
- **RQ2:** Can our approach maintain efficacy when applied to LMMs with a small amount of data? (Challenge 1)
- **RQ3:** Does minimizing redundancy in one stage suffice for satisfactory performance? (Challenge 2)
- **RQ4:** How does the performance compare between iterative pruning and one-shot pruning? (Challenge 2)
- **RQ5:** In our specific task, does employing hard label distillation adversely affect performance? (Challenge 3)
- **RQ6:** What is the impact of integrating pairwise loss on the model’s overall performance? (Challenge 3)

### 4.1 Datasets

Initially, we sought a suitable public dataset but were unable to locate any that were pertinent to our specific requirements. To advance real-world deployment, we extracted some real-world advertising data from Alipay and compiled a dataset, referred to as the Multimodal Advertisement Auditing Dataset (MAAD), designed to enable the pruning and distillation of AntGMM. We are currently anonymizing user information within MAAD to safeguard user privacy, and we are also undergoing a legal review to ensure compliance with relevant regulations. The release of the MAAD dataset is scheduled for about **February**, with the aim of contributing to



**Figure 5: A data sample from the dataset. It involves an advertisement image accompanied by a Chinese text segment. The text includes a carefully constructed prompt, possible assistant details, and a classification description of the advertisement. Some sensitive information has been processed.**

the wider research community’s efforts in LMMs’ applications. As shown in Figure 5, for multimodal audition scenarios, each data entry in our dataset comprises an image, a question, and an answer. In our study, we meticulously crafted prompts to leverage large models for our specific scenario. Our dataset encompasses 12,000 training samples and 3,000 test samples. Specifically, our data is composed of five distinct tasks: recognition of advertisement background color, identification of manifestations, classification of specific advertisement content, recognition of advertisement logos, and identification of advertisement styles. Each task is designed to probe a different aspect of the model’s capability to understand and process visual information pertaining to advertisements. This paper evaluated all tasks using **classification accuracy** as the metric.

### 4.2 Implementation Details

For the compression of AntGMM, a single process can be conducted on one A100 GPU. All our experiments were carried out on a machine equipped with eight A100s. Our inference time was assessed on a single A10 GPU. We employed the AdaW optimizer with a learning rate of  $3e-5$ . Drawing inspiration from the fine-tuning approach of LLaMA, we implemented a gradient schedule strategy using the cosine function. For the importance calculation during pruning and the knowledge distillation, we both utilized the entire training set of 12k samples. Our batch size was set to 1024. Regarding the parameters in our algorithm, we reduced the number of blocks by  $n_b = 4$  at each pruning iteration, with a maximum reduction of  $N_{blocks} = 40$  blocks. The intermediate-module layer dimension of the FFN was reduced by  $n_h^{(FFN)} = 768$  at each iteration, with a maximum reduction of  $N_{inter}^{(FFN)} = 6144$ . The intermediate-module layer dimension of attention was reduced by  $n_h^{(Att)} = 96$  at each iteration, with a maximum reduction of  $N_{inter}^{(Att)} = 768$ . The input/output dimensions were reduced by  $n_d = 96$  at each iteration, with a maximum reduction of  $N_{input} = 768$ . We set the maximum tolerance for the effect degradation to  $\alpha = 0.15$ . After each pruning iteration, we conducted distillation for  $E = 4$  epochs.

### 4.3 RQ1: Overall Performance

In this study, we applied our optimization framework to the AntGMM model, achieving substantial improvements. As detailed in Table 2,

**Table 2: Overall Model Performance**

Model	Size (B)	Inference Time on A10 (samples/s)	Color	Manifestations	Content	Logo	Style	Overall Accuracy
Original AntGMM	5.4	1.38	0.932	0.967	0.934	0.975	0.833	0.928
After Block Pruning	0.9	6.01	0.923	0.951	0.925	0.966	0.802	0.914
After Inter-Module Pruning	0.6	6.70	0.924	0.968	0.931	0.977	0.806	0.920
After Input/Output Pruning	0.3	7.62	0.920	0.971	0.916	0.981	0.825	0.923

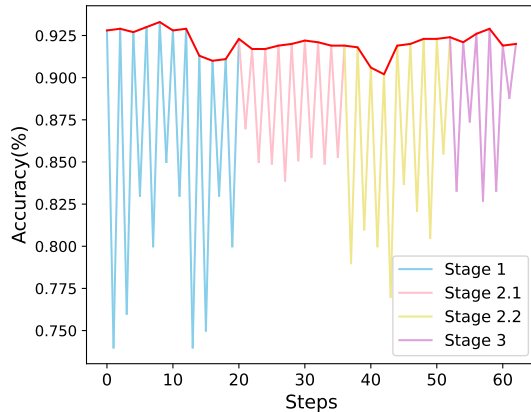


**Figure 6:** We present the results of each step, with a particular emphasis on the evaluation that pruning and distillation were separated into two steps in this figure. After each pruning step, which reduces performance, a distillation step follows to recover and enhance the performance throughout the process. The red line represents the overall performance variations where pruning and distillation are combined as one step throughout the entire process.

our method markedly reduced the model’s parameter count by approximately 18 times, from 5.4 billion to 0.3 billion. This reduction was accompanied by a significant increase in inference efficiency on the A10 processor, with a performance boost from 1.38 to 7.62 samples per second, which constitutes an enhancement of roughly 7.7 times. Despite this considerable decrease in parameters, the model’s performance on the test dataset remained robust without a significant decline. Notably, task-specific performance showed an uptick, with accuracy in Manifestations rising from 0.967 to 0.971 and in Logo recognition from 0.975 to 0.981. Block pruning played a pivotal role in these improvements, significantly reducing the parameter count to 0.9 billion and increasing inference efficiency to 6.01 samples per second.

Figure 6 illustrates the critical role of distillation in recuperating performance post-pruning. Following each pruning phase, which initially diminishes performance, a subsequent distillation phase is employed to recover and even augment performance. The pruning of intermediate-module dimensions in the FFN and the input/output dimensionality had a smaller impact on performance, as there is less fluctuation in these stages compared to others. In the other

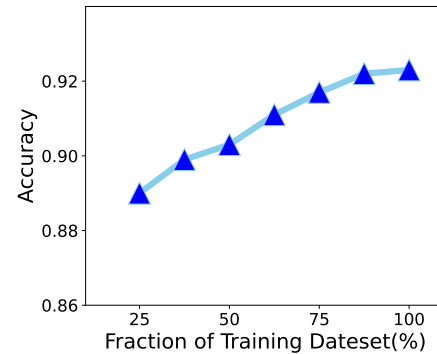


**Figure 7:** Correlation between sample size and performance.

two stages, performance was still effectively mitigated through distillation. Our method not only significantly reduced the number of parameters in the model and improved inference efficiency but also maintained model performance across most tasks and even enhanced it in specific tasks.

#### 4.4 RQ2: Training Samples and Performance

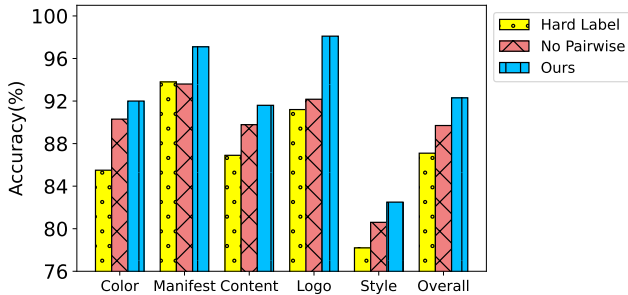
We also conducted a comprehensive analysis of the correlation between the final performance and the distillation sample size. The results depicted in the illustrated Figure 7 demonstrate a strong positive correlation between the sample size and the final compression effect of the model. Interestingly, it was observed that even with a sample size as small as 3k, desirable outcomes can be achieved. However, it is worth noting that a sample size of 12k proves to be sufficient in yielding results comparable to the original AntGMM. Consequently, the model that was eventually deployed online employed a sample size of 12k.

#### 4.5 RQ3: Only One Level Pruning

We also examined a single-stage pruning method, focusing on reducing individual redundancies rather than a collective approach to model compression. Referencing Table 3, pruning solely within the FFN of the intermediate module resulted in a significant drop in accuracy to 0.785. The effect was even more dramatic when pruning targeted only the intermediate-module dimensions of attention layers or the input/output dimensions, leading to a steep decline in performance. In particular, pruning just the input/output dimensions led to an accuracy of merely 0.061. These findings emphasize the high sensitivity of both the intermediate-module of attention

**Table 3: Comparison of Pruning Methods**

Model	Model Size (B)	Inference Time in A10 (samples/s)	Accuracy
Block Pruning Only	0.7	7.93	0.903
Inter-Module(FFN) Pruning Only	2.2	2.11	0.785
Inter-Module(Att) Pruning Only	3.8	1.87	0.080
Input/Output Pruning Only	0.6	1.95	0.061
Block Pruning Only (One-shot)	0.7	7.93	0.863
Inter-Module(FFN) Pruning Only (One-shot)	2.2	2.11	0.530
Inter-Module(Att) Pruning Only (One-shot)	3.8	1.87	0.076
Input/Output Pruning Only (One-shot)	0.6	1.95	0.033
All Stages (One-shot)	0.3	7.62	0.021
All Stages	0.3	7.62	0.923

**Figure 8: Efficacy of different distillation techniques on model accuracy. This figure depicts the comparative results of employing various distillation methods.**

and input/output dimensions to pruning. Therefore, our results suggest that pruning at a single level is inadequate for preserving an ideal balance between model size and performance during LMM compression, highlighting the limitations of single-stage pruning.

#### 4.6 RQ4: One-shot Pruning vs. Gradual Pruning

In addition, we also investigated the one-shot pruning approach, aiming for immediate attainment of the desired model structure followed by distillation. The findings highlighted the essential nature of our step-by-step pruning method. As shown in Table 3, one-shot pruning significantly impaired model performance to the degree that subsequent distillation could not recover. There was apparent in the sharp decline in accuracy, for example, from 0.785 to 0.530 in the one-time pruning of the FFN. Interestingly, the one-shot pruning of dimensions within the intermediate-module dimension of the attention or the input/output dimension proved the most harmful to performance. This is consistent with the findings of the only one-level pruning experiments. These results underscore the importance of careful, phased compression in LMM to preserve the model’s performance integrity.

#### 4.7 RQ5 & RQ6: Distillation Ablation

We also compared different distillation methods, as shown in Table 4 and Figure 8. We observed that when the pairwise loss was not used, the accuracy achieved was 0.871. However, our proposed method outperformed both approaches, achieving an accuracy of 0.923. These findings indicate that incorporating the pairwise loss method significantly enhances the distillation process, leading to

**Table 4: Comparison of Distillation Methods**

	No Pair-wise loss	Hard label Distillation	Ours
Accuracy	0.871	0.897	0.923

higher accuracy compared to not using the pairwise loss. Hence, our method demonstrates its effectiveness in improving the performance of the distillation process. Interestingly, we also explored the utilization of hard labels during the distillation process, where the labels from the dataset are employed as supplementary supervision information. However, our findings revealed that employing solely the outputs of the larger model as soft labels resulted in significant improvements in model performance.

## 5 ONLINE IMPROVEMENT

Compressed AntGMM with our method was deployed online at the end of September. Compared to the direct application of AntGMM, our method witnessed a marginal decrease in the seven-day average accuracy by 0.8%; however, it significantly reduced the service latency from approximately **700ms to 90ms**. In contrast to approaches not employing LMM, our model demonstrated an 18% increase in the seven-day average accuracy while incurring a mere 5ms increase in latency.

## 6 RELATED WORKS

**Large Multimodal Model.** Advancements in LMMs, such as BLIP-2’s use of frozen FlanT5 models for visual features extraction [21], MiniGPT-4’s integration of a visual encoder with Vicuna LLM and ChatGPT captions [48], and LLaVA’s combination of a visual encoder output with LLaMA [20], have significantly enhanced vision-language tasks. Additionally, mPLUG-Owl introduces a modular training paradigm that surpasses MiniGPT-4 and LLaVA in understanding instructions and visuals [42]. Our company’s current version of AntGMM adopts a structure based on BLIP-2, and we are exploring other approaches and employing various techniques to improve our service quality.

**Large Model Compression.** Large model compression techniques include network pruning [10, 26, 33], knowledge distillation [12, 22, 32], and quantization [7, 24, 39], supplemented by methods like early exit [5] and dynamic token reduction [5]. Our research focuses on language model pruning, particularly structural pruning and distillation. Structural pruning, involving the removal of entire filters for hardware efficiency, utilizes various methods like l1-dependent pruning [44], first-order importance estimation [14], and Hessian-based estimation [26, 38]. Concerning the pruning unit in structural pruning, some works consider the entire layer [8] as the minimal unit, while others regard multi-head attention [37] or the feed-forward layers [27] as the fundamental structures for pruning. We adopt a multi-stage approach to reduce redundancy across various levels.



## 7 CONCLUSION AND DISCUSSION

The integration of AntGMM within AntGroup’s digital infrastructure has underscored the transformative influence of Large Multimodal Models in bolstering task precision across various industrial applications. Despite this success, the initial deployment highlighted challenges, notably increased latency and significant energy consumption, underscoring the need for sustainable AI practices. Our multi-stage model compression strategy response effectively addressed these issues, striking a balance between performance and efficiency. This approach, tailored for generative LMMs, has proven its merit over several months’ online period, maintaining high-performance standards while achieving a reduction in latency and operational costs. This venture into sustainable model deployment solidifies AntGroup’s position as a leader in industrial AI applications and reflects our dedication to Green AI principles. Our work is an industry framework for responsible AI applications that prioritize ecological integrity without sacrificing service quality.

## REFERENCES

- [1] Jie An, Zhengyuan Yang, Linjie Li, Jianfeng Wang, Kevin Lin, Zicheng Liu, Lijuan Wang, and Jiebo Luo. 2023. OpenLEAF: Open-Domain Interleaved Image-Text Generation and Evaluation. *arXiv preprint arXiv:2310.07749* (2023).
- [2] Sajid Anwar, Kyuyeon Hwang, and Wonyong Sung. 2017. Structured pruning of deep convolutional neural networks. *ACM Journal on Emerging Technologies in Computing Systems (JETC)* 13, 3 (2017), 1–18.
- [3] Jinze Bai, Shuai Bai, Yunfei Chu, Zeyu Cui, Kai Dang, Xiaodong Deng, Yang Fan, Wenbin Ge, Yu Han, Fei Huang, et al. 2023. Qwen technical report. *arXiv preprint arXiv:2309.16609* (2023).
- [4] Tom Brown, Benjamin Mann, Nick Ryder, Melanie Subbiah, Jared D Kaplan, Prafulla Dhariwal, Arvind Neelakantan, Pranav Shyam, Girish Sastry, Amanda Askell, et al. 2020. Language models are few-shot learners. *Advances in neural information processing systems* 33 (2020), 1877–1901.
- [5] Luciano Del Corro, Allie Del Giorno, Sahaj Agarwal, Bin Yu, Ahmed Awadallah, and Subhabrata Mukherjee. 2023. SkipDecode: Autoregressive Skip Decoding with Batching and Caching for Efficient LLM Inference. *arXiv preprint arXiv:2307.02628* (2023).
- [6] Mohammad Delsoz, Hina Raja, Yeganeh Madadi, Anthony A Tang, Barbara M Wirotko, Malik Y Kahook, and Siamak Yousefi. 2023. The Use of ChatGPT to Assist in Diagnosing Glaucoma Based on Clinical Case Reports. *Ophthalmology and Therapy* (2023), 1–12.
- [7] Tim Dettmers, Mike Lewis, Younes Belkada, and Luke Zettlemoyer. 2022. Llm.int8(): 8-bit matrix multiplication for transformers at scale. *arXiv preprint arXiv:2208.07339* (2022).
- [8] Angela Fan, Edouard Grave, and Armand Joulin. 2019. Reducing transformer depth on demand with structured dropout. *arXiv preprint arXiv:1909.11556* (2019).
- [9] Gongfan Fang, Xinyin Ma, Mingli Song, Michael Bi Mi, and Xinchao Wang. 2023. DepGraph: Towards Any Structural Pruning. *The IEEE/CVF Conference on Computer Vision and Pattern Recognition* (2023).
- [10] Elias Frantar and Dan Alistarh. 2023. SparseGPT: Massive Language Models Can Be Accurately Pruned in One-Shot. (2023).
- [11] Mitchell A Gordon, Kevin Duh, and Nicholas Andrews. 2020. Compressing BERT: Studying the Effects of Weight Pruning on Transfer Learning. *ACL 2020* (2020), 143.
- [12] Yuxian Gu, Li Dong, Furu Wei, and Minlie Huang. 2023. Knowledge Distillation of Large Language Models. *arXiv preprint arXiv:2306.08543* (2023).
- [13] Geoffrey Hinton, Oriol Vinyals, and Jeff Dean. 2015. Distilling the knowledge in a neural network. *arXiv preprint arXiv:1503.02531* (2015).
- [14] Lu Hou, Zhiqi Huang, Lifeng Shang, Xin Jiang, Xiao Chen, and Qun Liu. 2020. Dynabert: Dynamic bert with adaptive width and depth. *Advances in Neural Information Processing Systems* 33 (2020), 9782–9793.
- [15] Xiaoqi Jiao, Yichun Yin, Lifeng Shang, Xin Jiang, Xiao Chen, Linlin Li, Fang Wang, and Qun Liu. 2020. TinyBERT: Distilling BERT for Natural Language Understanding. In *EMNLP 2020*. 4163–4174.
- [16] Sehoon Kim, Amir Gholami, Zhewei Yao, Michael W Mahoney, and Kurt Keutzer. 2021. I-bert: Integer-only bert quantization. In *International conference on machine learning*. PMLR, 5506–5518.
- [17] Se Jung Kwon, Dongsoo Lee, Byeongwook Kim, Parichay Kapoor, Baeseong Park, and Gu-Yeon Wei. 2020. Structured compression by weight encryption for unstructured pruning and quantization. In *Proceedings of the IEEE/CVF Conference on Computer Vision and Pattern Recognition*. 1909–1918.
- [18] Jaeho Lee, Sejun Park, Sangwoo Mo, Sungsoo Ahn, and Jinwoo Shin. 2020. Layer-adaptive sparsity for the magnitude-based pruning. *arXiv preprint arXiv:2010.07611* (2020).
- [19] Bingbing Li, Zhenglun Kong, Tianyun Zhang, Ji Li, Zhengang Li, Hang Liu, and Caiwen Ding. 2020. Efficient transformer-based large scale language representations using hardware-friendly block structured pruning. *arXiv preprint arXiv:2009.08065* (2020).
- [20] Chunyuan Li, Cliff Wong, Sheng Zhang, Naoto Usuyama, Haotian Liu, Jianwei Yang, Tristan Naumann, Hoifung Poon, and Jianfeng Gao. 2023. Llava-med: Training a large language-and-vision assistant for biomedicine in one day. *arXiv preprint arXiv:2306.00890* (2023).
- [21] Junnan Li, Dongxu Li, Silvio Savarese, and Steven Hoi. 2023. Blip-2: Bootstrapping language-image pre-training with frozen image encoders and large language models. *arXiv preprint arXiv:2301.12597* (2023).
- [22] Chen Liang, Haoming Jiang, Zheng Li, Xianfeng Tang, Bin Yin, and Tuo Zhao. 2023. Homodistil: Homotopic task-agnostic distillation of pre-trained transformers. *arXiv preprint arXiv:2302.09632* (2023).
- [23] Zejian Liu, Fanrong Li, Gang Li, and Jian Cheng. 2021. EBERT: Efficient BERT inference with dynamic structured pruning. In *Findings of the Association for Computational Linguistics: ACL-IJCNLP 2021*. 4814–4823.
- [24] Zechun Liu, Barlas Ogu, Changsheng Zhao, Ernie Chang, Pierre Stock, Yashar Mehdad, Yangyang Shi, Raghuraman Krishnamoorthi, and Vikas Chandra. 2023. LLM-QAT: Data-Free Quantization Aware Training for Large Language Models. *arXiv preprint arXiv:2305.17888* (2023).
- [25] Hanwen Luo, Yudong Li, Xiaodong Wang, and Yuqing Zhang. 2020. Knowledge distillation and data augmentation for NLP light pre-trained models. In *Journal of Physics: Conference Series*, Vol. 1651. IOP Publishing, 012043.
- [26] Xinyin Ma, Gongfan Fang, and Xinchao Wang. 2023. LLM-Pruner: On the Structural Pruning of Large Language Models. In *Advances in Neural Information Processing Systems*.
- [27] JS McCarley, Rishav Chakravarti, and Avirup Sil. 2019. Structured pruning of a bert-based question answering model. *arXiv preprint arXiv:1910.06360* (2019).
- [28] Pavlo Molchanov, Arun Mallya, Stephen Tyree, Iuri Frosio, and Jan Kautz. 2019. Importance estimation for neural network pruning. In *Proceedings of the CVPR*. 11264–11272.
- [29] Alec Radford, Jong Wook Kim, Chris Hallacy, Aditya Ramesh, Gabriel Goh, Sandhini Agarwal, Girish Sastry, Amanda Askell, Pamela Mishkin, Jack Clark, et al. 2021. Learning transferable visual models from natural language supervision. In *International conference on machine learning*. PMLR, 8748–8763.
- [30] Sheng Shen, Zhen Dong, Jiayu Ye, Linjian Ma, Zhewei Yao, Amir Gholami, Michael W Mahoney, and Kurt Keutzer. 2020. Q-bert: Hessian based ultra low precision quantization of bert. In *Proceedings of the AAAI Conference on Artificial Intelligence*, Vol. 34. 8815–8821.
- [31] Jonathon Shlens. 2014. Notes on kullback-leibler divergence and likelihood. *arXiv preprint arXiv:1404.2000* (2014).
- [32] Kumar Shridhar, Alessandro Stolfo, and Mrinmaya Sachan. 2023. Distilling reasoning capabilities into smaller language models. In *Findings of the Association for Computational Linguistics: ACL 2023*. 7059–7073.
- [33] Mingjie Sun, Zhuang Liu, Anna Bair, and J Zico Kolter. 2023. A Simple and Effective Pruning Approach for Large Language Models. *arXiv preprint arXiv:2306.11695* (2023).
- [34] Siqi Sun, Yu Cheng, Zhe Gan, and Jingjing Liu. 2019. Patient Knowledge Distillation for BERT Model Compression. In *(EMNLP-IJCNLP)*. Association for Computational Linguistics.
- [35] Aaquib Syed, Phillip Huang Guo, and Vijaykaarti Sundarapandian. 2023. Prune and Tune: Improving Efficient Pruning Techniques for Massive Language Models. (2023).
- [36] Hugo Touvron, Louis Martin, Kevin Stone, Peter Albert, Amjad Almahairi, Yasmine Babaei, Nikolay Bashlykov, Soumya Batra, Prajwal Bhargava, Shrutu Bhosale, et al. 2023. Llama 2: Open foundation and fine-tuned chat models. *arXiv preprint arXiv:2307.09288* (2023).
- [37] Elena Voita, David Talbot, Fedor Moiseev, Rico Sennrich, and Ivan Titov. 2019. Analyzing multi-head self-attention: Specialized heads do the heavy lifting, the rest can be pruned. *arXiv preprint arXiv:1905.09418* (2019).
- [38] Chaoqi Wang, Roger Grosse, Sanja Fidler, and Guodong Zhang. 2019. Eigendamage: Structured pruning in the kronecker-factored eigenbasis. In *International conference on machine learning*. PMLR, 6566–6575.
- [39] Guangxuan Xiao, Ji Lin, Mickael Seznec, Hao Wu, Julien Demouth, and Song Han. 2023. Smoothquant: Accurate and efficient post-training quantization for large language models. In *ICML*. PMLR, 38087–38099.
- [40] Canwen Xu and Julian McAuley. 2023. A survey on model compression and acceleration for pretrained language models. In *Proceedings of the AAAI Conference on Artificial Intelligence*, Vol. 37. 10566–10575.
- [41] Aiyuan Yang, Bin Xiao, Bingning Wang, Borong Zhang, Chao Yin, Chenxu Lv, Da Pan, Dian Wang, Dong Yan, Fan Yang, et al. 2023. Baichuan 2: Open large-scale language models. *arXiv preprint arXiv:2309.10305* (2023).

[42] Qinghao Ye, Haiyang Xu, Guohai Xu, Jiabo Ye, Ming Yan, Yiyang Zhou, Junyang Wang, Anwen Hu, Pengcheng Shi, Yaya Shi, et al. 2023. mplug-owl: Modularization empowers large language models with multimodality. *arXiv preprint arXiv:2304.14178* (2023).

[43] Zixuan Yi, Zijun Long, Iadh Ounis, Craig Macdonald, and Richard McCreadie. 2023. Large Multi-modal Encoders for Recommendation. *arXiv preprint arXiv:2310.20343* (2023).

[44] Ofir Zafrir, Ariel Larey, Guy Boudoukh, Haihao Shen, and Moshe Wasserblat. 2021. Prune once for all: Sparse pre-trained language models. *arXiv preprint arXiv:2111.05754* (2021).

[45] Yihan Zeng, Chenhan Jiang, Jiageng Mao, Jianhua Han, Chaoqiang Ye, Qingqiu Huang, Dit-Yan Yeung, Zhen Yang, Xiaodan Liang, and Hang Xu. 2023. CLIP2: Contrastive Language-Image-Point Pretraining from Real-World Point Cloud Data. In *Proceedings of the CVPR*. 15244–15253.

[46] Zhenyu Zhang, Xiaobo Shu, Bowen Yu, Tingwen Liu, Jiapeng Zhao, Quangang Li, and Li Guo. 2020. Distilling knowledge from well-informed soft labels for neural relation extraction. In *Proceedings of the AAAI*, Vol. 34. 9620–9627.

[47] You Zhou, Xiujing Lin, Xiang Zhang, Maolin Wang, Gangwei Jiang, Huakang Lu, Yupeng Wu, Kai Zhang, Zhe Yang, Kehang Wang, et al. 2023. On the Opportunities of Green Computing: A Survey. *arXiv preprint arXiv:2311.00447* (2023).

[48] Deyao Zhu, Jun Chen, Xiaoqian Shen, Xiang Li, and Mohamed Elhoseiny. 2023. Minigt-4: Enhancing vision-language understanding with advanced large language models. *arXiv preprint arXiv:2304.10592* (2023).

[49] Xunyu Zhu, Jian Li, Yong Liu, Can Ma, and Weiping Wang. 2023. A survey on model compression for large language models. *arXiv preprint arXiv:2308.07633* (2023).

Text	Image	Label	Prediction of Compressed AnIGMM
### Human: 结合标题描述图片商品的行业类别,标题为“米德伦雅牛津布背包 / 1个”,G:G#MEMBER#xxx, MEMBER, xxx,米格伦雅牛津布背包/个, http://alipayobjects/xxx/xx/file/xxx/### Assistant: [gMASK]		电商日用百货+纸品清洁	电商配饰
### Human: 结合标题描述图片商品的行业类别,标题为“居家必备-智能扫地机,宠物大额优惠券,领券下单,丁乙家居,扫地机,202100xxx,” ### Assistant: [gMASK]		电商家具	电商日用百货+纸品清洁
### Human: 结合标题描述图片商品的行业类别,标题为“古康自带4线迷你1W毫安充电宝 多色多规格,G:G#MEMBER#2023 xxx, MEMBER, 20230xxx, 古康自带4线迷你1W毫安充电宝 多色多规格, http://alipay/xx/Axxx, ”###Assistant: [gMASK]		电商日用百货+纸品清洁	电商消费电子

Figure 9: Some bad caeses. Some sensitive information has been processed.

### A CASE STUDY

As shown in Figure 9, it is noteworthy that we selected several misclassified samples and found that many of the categorization errors are related to our ambiguous labeling, which are also difficult for humans to discern. Nonetheless, it is important to highlight that such classification discrepancies are unlikely to substantially affect real-world business applications.

### B MODEL SIZE AND STEPS

As depicted in the Figure 10, we observe the variation in model size with respect to the number of steps. It is evident that the parameter count decreases most rapidly during the block pruning phase. This is followed by a more gradual reduction in the inter-module stage, and a modest decrease is also noted in the input/output parameters.

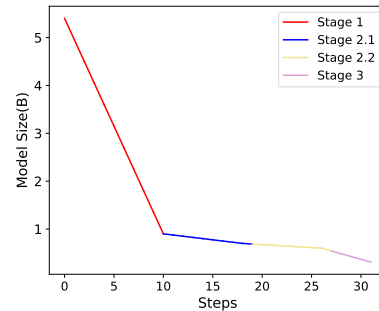


Figure 10: Correlation between model size and step.

### C MODEL SIZE AND PERFORMANCE

The Figure 11 illustrates the relationship between model size and performance. To enhance clarity, we have applied a log2 transformation to the values representing model size. Our observations indicate that generally, a smaller model correlates with reduced performance within a given phase. However, there are instances of significant performance improvement, suggesting an absence of a consistent pattern.

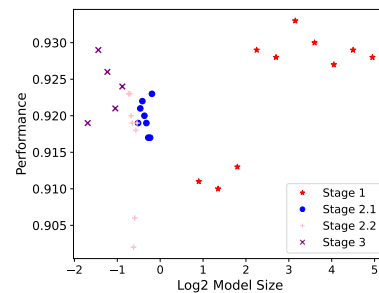


Figure 11: Correlation between model size and performance.

### D REAL WORD DISPLAY

Figure 12 showcases real-world multimodal advertisements in Ali-pay that are subject to auditing.

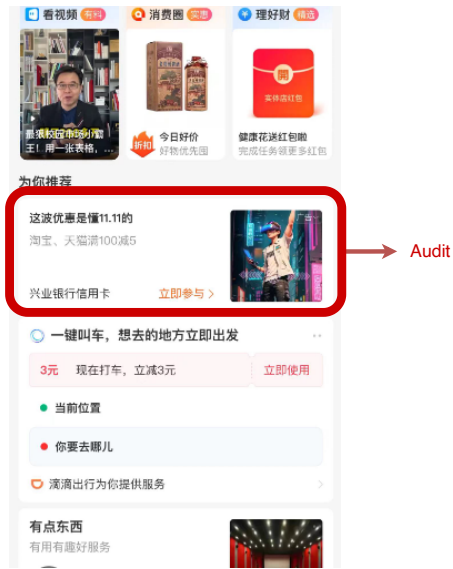


Figure 12: Real-world Alipay interface. The advertisements to be audited are enclosed within red boxes.